Monatshefte für Chemie 133, 919–929 (2002)

Monatshefte für Chemie
Chemical Monthly

EXAFS Investigations on Nanocomposites Composed of Surface-Modified Zirconium and Zirconium/Titanium Mixed Metal Oxo Clusters and Organic Polymers

Guido Kickelbick[1,*], **Martin P. Feth**[2], **Helmut Bertagnolli**[2], **Bogdan Moraru**[1], **Gregor Trimmel**[1], and **Ulrich Schubert**[1]

[1] Institut für Materialchemie, Technische Universität Wien, A-1060 Wien, Austria
[2] Institut für Physikalische Chemie, Universität Stuttgart, D-70550 Stuttgart, Germany

Summary. The surface-modified oxometallate clusters $Zr_6(OH)_4O_4(OMc)_{12}$, $Ti_4Zr_4O_6(OBu)_4(OMc)_{16}$, and $Ti_2Zr_4O_4(OBu)_2(OMc)_{14}$ (OMc = methacrylate) as well as their nanocomposites with polystyrene, poly(methacrylic acid) and poly(methyl methacrylate) were investigated by EXAFS. Studies on the nanocomposites revealed that the structure of the cluster core is retained in the hybrid materials.

Keywords. Clusters; EXAFS spectroscopy; Nanostructures; Polymerizations.

Introduction

The formation of nanocomposites embedding inorganic nanostructures in organic polymers is one of the promising methods to get new functional materials [1–5]. Phase separation is a major problem that often occurs in this kind of materials, which can be avoided by covalent bonding between the inorganic phase and the organic polymer. The attachment of organic groups with crosslinking capability onto the surface of the inorganic species allows incorporating the inorganic component by polymerization reactions. This has been proved, for example, by the surface modification of silica particles [6–11]. To expand the properties of the composite materials, new inorganic components have to be included. We have shown in earlier work that it is possible to prepare surface-modified clusters of zirconium and titanium as well as mixed zirconium–titanium systems by an *in situ* functionalization during formation of the clusters [3, 12–17]. The prepared clusters with diameters between about 0.7 and 1.7 nm of the inorganic core were incorporated in a variety of polymers, and the resulting crosslinked materials were characterized by TGA, DSC, SAXS, and NMR measurements as well as by their swelling behaviour [18, 19]. From all these methods it was not totally clear whether the cluster core was

* Corresponding author. E-mail: kickelgu@mail.zserv.tuwien.ac.at

retained in the composites. This paper reports on extended X-ray absorption fine structure (EXAFS) analyses as a powerful tool for the investigation of the local atomic environment of atoms, independent of the state of the sample [20] which was carried out on some metal oxo-clusters in organic polymers.

Results and Discussions

EXAFS investigations of the Zr_6 cluster at the Zr–K edge

The reaction of $Zr(OPr)_4$ in propanol with a 4-fold excess of methacrylic acid forms the cluster $Zr_6(OH)_4O_4(OMc)_{12}$. It consists of an octahedral $Zr_6O_4(OH)_4$ core in which the triangular faces of the Zr_6 octahedron are capped by either μ_3-O or μ_3-OH groups. Chelating and bridging methacrylate ligands saturate the remaining Zr coordination sites [12]. Inspection of the crystal structure shows that the double bonds on the surface of the cluster are fully accessible for further chemical reactions. The diameter of the cluster core of this structurally well-defined core-shell nanoparticle is approximately 0.5 nm, and that of the whole particle 1.4 nm. Nanocomposite materials were obtained by crosslinking the cluster with methyl methacrylate and methacrylic acid (50-fold molar excess of the monomer) in a free radical polymerization initiated by dibenzoyl peroxide in a benzene solution [19]. One of the major questions regarding these materials is whether the cluster was incorporated in the polymer without break-up of its structure. Results from SAXS measurements of the materials showed that the microstructure of the cluster-doped polymers can be described by a hard-sphere packing of identical spherical clusters. However, SAXS could not provide information about the molecular structure of the inorganic moiety, and therefore EXAFS investigations were carried out. The results of the EXAFS analysis are

Table 1. Structural parameters of the $Zr_6(OH)_4O_4(OMc)_{12}$ cluster (crystalline and copolymerized with methyl methacrylate and methacrylic acid) as determined from the Zr–K edge EXAFS spectrum; the coordination numbers were fixed according to the averaged crystallographic values

	[a]	r/Å	N	σ/Å	ΔE_0/eV	k-range/Å^{-1} Fit-index
Zr_6 cluster, crystalline	Zr–O	2.09±0.02	2	0.081±0.012	21.3	3.10–16.20
	Zr–O	2.24±0.02	6	0.093±0.014		32.0
	Zr–Zr	3.52±0.04	4	0.076±0.010		
Zr_6 cluster in poly-(methyl-methacrylate)	Zr–O	2.10±0.02	2	0.066±0.011	20.8	3.00–16.20
	Zr–O	2.24±0.02	6	0.085±0.013		31.3
	Zr–Zr	3.53±0.04	4	0.075±0.010		
Zr_6 cluster in polymethacrylate	Zr–O	2.09±0.02	2	0.071±0.010	21.5	3.00–16.20
	Zr–O	2.23±0.02	6	0.084±0.013		35.2
	Zr–Zr	3.52±0.04	4	0.073±0.010		
Zr_6 cluster, XRD [12]	Zr–O	2.07	2			
	Zr–O	2.21	6			
	Zr–Zr	3.51	4			

[a] Absorber-backscatterer distance r, coordination number N, *Debye-Waller* factor σ, shift of the energy threshold energy ΔE_0, fit-index R

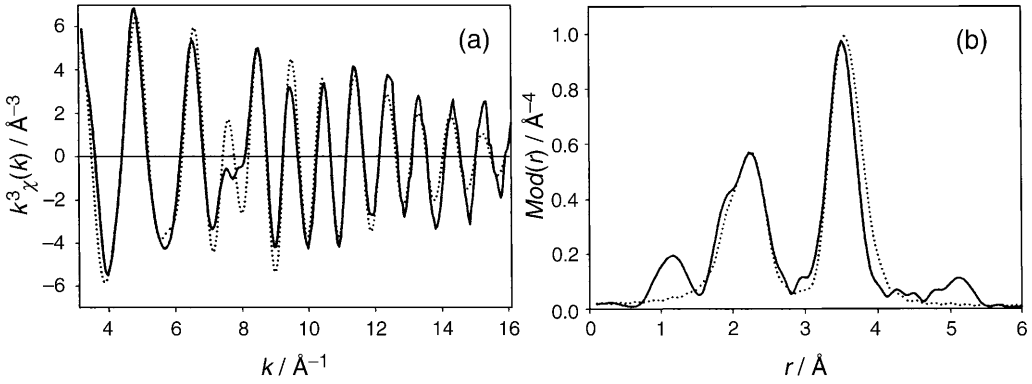

Fig. 1. Experimental (solid line) and calculated (dotted line) $k^3\chi(k)$ function (a) and their *Fourier* transforms (b) of the $Zr_6(OH)_4O_4(OMc)_{12}$ cluster at the Zr–K edge

shown in Table 1. In a first step the EXAFS data for the crystalline system were compared with the data of the structurally characterized cluster [12]. The crystal structure reveals that each Zr atom in the cluster has a first coordination sphere formed by two μ_3-O, two μ_3-OH, and four methacrylic acid O atoms. As can be seen from the *Fourier* transformed EXAFS function of the pure Zr_6 cluster (Fig. 1b), these three different oxygen types of the first coordination sphere appear as a not well-resolved double peak. The other very intense peak at a distance of about 3.5 Å can be related to zirconium backscatter. In the EXAFS analysis of the experimental k^3-weighted $\chi(k)$ function (Fig. 1a), a three-shell model can be fitted. In this analysis the coordination numbers were set to the known averaged crystallographic values [12]. The first Zr–O distance was found at 2.09 Å ($N=2$), the second at 2.24 Å ($N=6$). The Zr–Zr distance is at 3.52 Å ($N=4$). The structural parameters of the pure cluster determined by EXAFS are in very good agreement with those found from the single crystal XRD [12]. For the analysis of the nanocomposites EXAFS data, the same model for the coordination numbers was used. The hybrid materials, poly(methacrylic acid) crosslinked by the cluster, showed also a good agreement with the data in the crystalline state (Fig. 2), even the *Debye-Waller*-like factor σ remained in the same order of magnitude. This means that in both cases the original cluster structure appears to be still present in

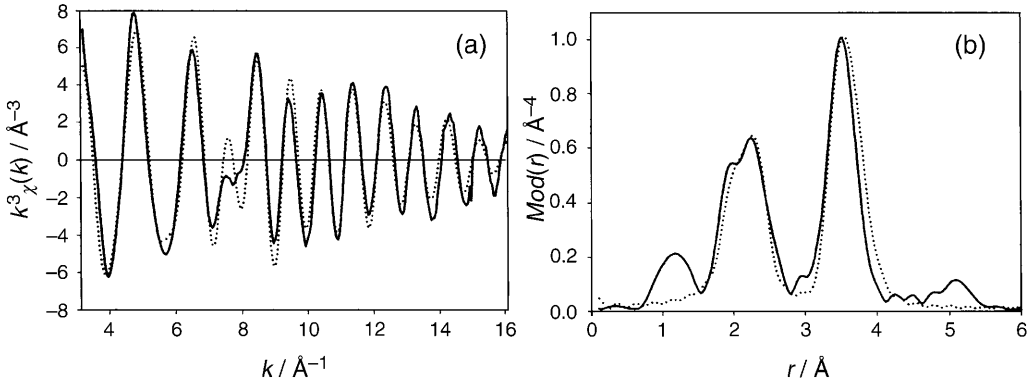

Fig. 2. Experimental (solid line) and calculated (dotted line) $k^3\chi(k)$ function (a) and their *Fourier* transforms (b) of the $Zr_6(OH)_4O_4(OMc)_{12}$ cluster in poly(methacrylic acid) at the Zr–K edge

the polymer matrix. Hence, a cleavage of the cluster by interaction with the monomers, which is a possible decomposition reaction already observed with other bidentate ligands [21] did not occur. This is a possible side reaction especially in

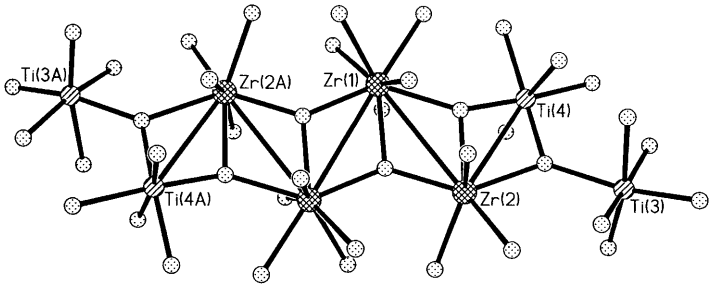

Fig. 3. Representation of the core of the $Ti_4Zr_4O_6(OBu)_4(OMc)_{16}$ cluster from X-ray structure analysis [16]

Table 2. Structural parameters of the $Ti_4Zr_4O_6(OBu)_4(OMc)_{16}$ cluster (pure as well as copolymerized with methacrylic acid (*MA*), methyl methacrylate (*MMA*), and styrene (*St*) in different ratios) as determined from the Zr–K edge EXAFS spectrum; the coordination numbers were fixed according to the averaged crystallographic values; for symbols, cf. Table 1

		r/Å	N	σ/Å	ΔE_0/eV	k-range/Å^{-1} Fit-index
Ti_4Zr_4 cluster,	Zr–O	2.20±0.02	7.5	0.086	19.9	3.20–14.30
crystalline	Zr–Ti	3.14±0.03	0.5	0.067		29.5
	Zr–Zr	3.53±0.04	1.5	0.088		
Ti_4Zr_4 cluster,	Zr–O	2.19±0.02	7.5	0.093	19.9	3.10–14.20
MA ratio 1:50	Zr–Ti	3.15±0.03	0.5	0.072		27.6
	Zr–Zr	3.52±0.04	1.5	0.099		
Ti_4Zr_4 cluster,	Zr–O	2.20±0.02	7.5	0.094	19.9	3.10–14.20
MA ratio 1:100	Zr–Ti	3.15±0.03	0.5	0.066		28.9
	Zr–Zr	3.53±0.04	1.5	0.097		
Ti_4Zr_4 cluster,	Zr–O	2.19±0.02	7.5	0.097	19.4	3.10–14.20
MMA ratio 1:50	Zr–Ti	3.17±0.03	0.5	0.077		27.3
	Zr–Zr	3.51±0.04	1.5	0.096		
Ti_4Zr_4 cluster,	Zr–O	2.19±0.02	7.5	0.096	20.1	3.20–14.30
MMA ratio 1:100	Zr–Ti	3.19±0.03	0.5	0.075		30.4
	Zr–Zr	3.50±0.04	1.5	0.105		
Ti_4Zr_4 cluster,	Zr–O	2.19±0.02	7.5	0.093	19.6	3.20–14.30
St ratio 1:50	Zr–Ti	3.18±0.03	0.5	0.076		27.9
	Zr–Zr	3.50±0.04	1.5	0.105		
Ti_4Zr_4 cluster,	Zr–O	2.19±0.02	7.5	0.093	19.7	3.20–14.30
St ratio 1:100	Zr–Ti	3.18±0.03	0.5	0.076		27.9
	Zr–Zr	3.50±0.04	1.5	0.108		
Ti_4Zr_4 cluster,	Zr–O	2.17	7.5			
XRD [16]	Zr–Ti	3.07	0.5			
	Zr–Zr	3.45	1.5			

the case of the methacrylic acid polymer with its free carboxylic acid groups. However, it cannot be excluded that surface methacrylate groups of the cluster exchange against pending groups from this polymer, which would not change the first coordination sphere around the Zr atoms.

EXAFS investigations of mixed Zr/Ti clusters at the Zr–K and Ti–K edge

Methacrylate-substituted mixed Zr/Ti clusters were synthesized by reaction of $Ti(OBu)_4$, $Zr(OBu)_4$, and methacrylic acid [16]. Depending on the Ti:Zr alkoxide ratio, different structures were obtained and characterized: $Ti_4Zr_4O_6(OBu)_4(OMc)_{16}$ at a 1:1 and $Ti_2Zr_4O_4(OBu)_2(OMc)_{14}$ at a 1:2 ratio. Both clusters show zigzag chains of $[ZrO_8]$ dodecahedra and $[TiO_6]$ octahedra building units. Contrary to the Zr_6 cluster, which can be best described as a spherical system, the metal chains in the mixed-metal compounds are arranged in an oblong shape. Particularly interesting for these compounds is the possibility to analyze the surroundings of both metal atoms due to the good X-ray absorption properties of both Zr and Ti.

Ti_4Zr_4 cluster

In $Ti_4Zr_4O_6(OBu)_4(OMc)_{16}$ the zigzag chain consists of four inner $[ZrO_8]$ dodecahedra and two $[TiO_6]$ octahedra condensed to both ends of this chain (Fig. 3).

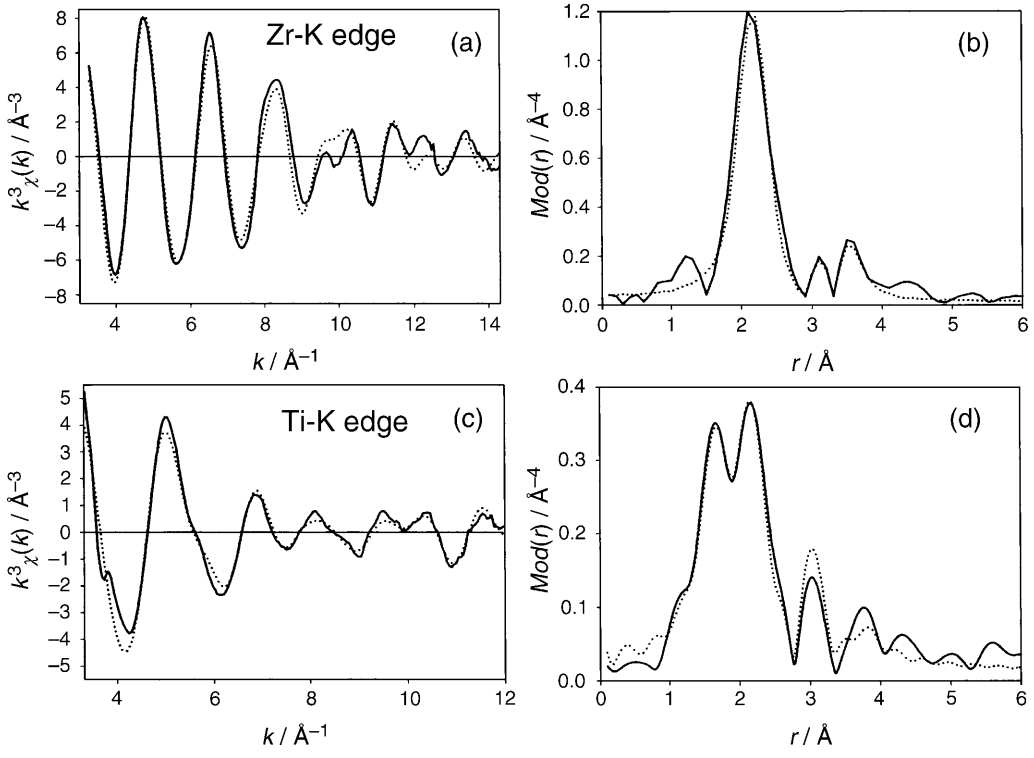

Fig. 4. Experimental (solid line) and calculated (dotted line) $k^3\chi(k)$ functions (a, c) and their *Fourier* transforms (b, d) of the pure $Ti_4Zr_4O_6(OBu)_4(OMc)_{16}$ cluster at the Zr–K (a, b) and Ti–K edge (c, d)

The average surrounding of a Zr atom in this cluster is best described by 7.5 O atoms at 2.17 Å, 0.5 Ti atoms at 3.07 Å, and 1.5 Zr atoms at 3.45 Å according to the molecular structure from single crystal X-ray diffraction experiments as can also be seen from the results of the Zr–K edge experiments (Table 2, Fig. 4). Non-integer numbers of atoms express that not every Zr atom has the same coordination sphere. The EXAFS data are in good agreement with the crystallographic data. However, compared to the Zr_6 cluster, the iterated bond lengths are somewhat longer, especially those obtained from Ti and Zr backscatter. This is a general observation in all mixed metal compounds. The origin of this small deviation is currently not clear. The results of the Zr–K edge were supported by Ti–K edge data (Table 3). The average surroundings of the Ti atoms based on the single crystal X-ray structure is best described by 2 O atoms in a distance of 1.83 Å, 4 O atoms at 2.04 Å, 0.5 Zr atoms at 3.07 Å, and 1 Ti atom at 3.45 Å. Analysis of the EXAFS

Table 3. Structural parameters of the $Ti_4Zr_4O_6(OBu)_4(OMc)_{16}$ cluster (pure as well as copolymerized with methacrylic acid (*MA*), methyl methacrylate (*MMA*), and styrene (*St*) in different ratios) as determined from the Ti–K edge EXAFS spectrum; the coordination numbers were fixed according to the averaged crystallographic values; for symbols, cf. Table 1

		r/Å	N	σ/Å	ΔE_0/eV	k-range/Å^{-1} Fit-index
Ti_4Zr_4 cluster,	Ti–O	1.84±0.02	2	0.090±0.014	15.8	3.30–12.00
crystalline	Ti–O	2.04±0.02	4	0.106±0.016		24.3
	Ti–Zr	3.13±0.03	0.5	0.079±0.015		
	Ti–Ti	3.51±0.04	1	0.095±0.013		
Ti_4Zr_4 cluster,	Ti–O	1.83±0.02	2	0.096±0.014	16.8	3.30–10.00
MA ratio 1:50	Ti–O	2.03±0.02	4	0.112±0.017		26.8
	Ti–Zr	3.14±0.03	0.5	0.112±0.016		
Ti_4Zr_4 cluster,	Ti–O	1.85±0.02	2	0.105±0.016	15.6	3.30–12.00
MA ratio 1:100	Ti–O	2.04±0.02	4	0.118±0.018		22.4
	Ti–Zr	3.14±0.03	0.5	0.084±0.015		
	Ti–Ti	3.49±0.04	1	0.117±0.017		
Ti_4Zr_4 cluster,	Ti–O	1.82±0.02	2	0.110±0.015	17.8	3.30–11.00
MMA ratio 1:50	Ti–O	2.01±0.02	4	0.119±0.017		30.7
	Ti–Zr	3.13±0.03	0.5	0.090±0.015		
Ti_4Zr_4 cluster,	Ti–O	1.84±0.02	2	0.098±0.015	16.0	3.30–12.00
St ratio 1:50	Ti–O	2.04±0.02	4	0.108±0.016		21.3
	Ti–Zr	3.16±0.03	0.5	0.082±0.015		
	Ti–Ti	3.50±0.04	1	0.107±0.016		
Ti_4Zr_4 cluster,	Ti–O	1.85±0.02	2	0.105±0.015	15.8	3.30–12.00
St ratio 1:100	Ti–O	2.04±0.02	4	0.115±0.017		25.0
	Ti–Zr	3.14±0.03	0.5	0.086±0.016		
	Ti–Ti	3.50±0.04	1	0.109±0.016		
Ti_4Zr_4 cluster,	Ti–O	1.83	2			
XRD [16]	Ti–O	2.04	4			
	Ti–Zr	3.07	0.5			
	Ti–Ti	3.45	1			

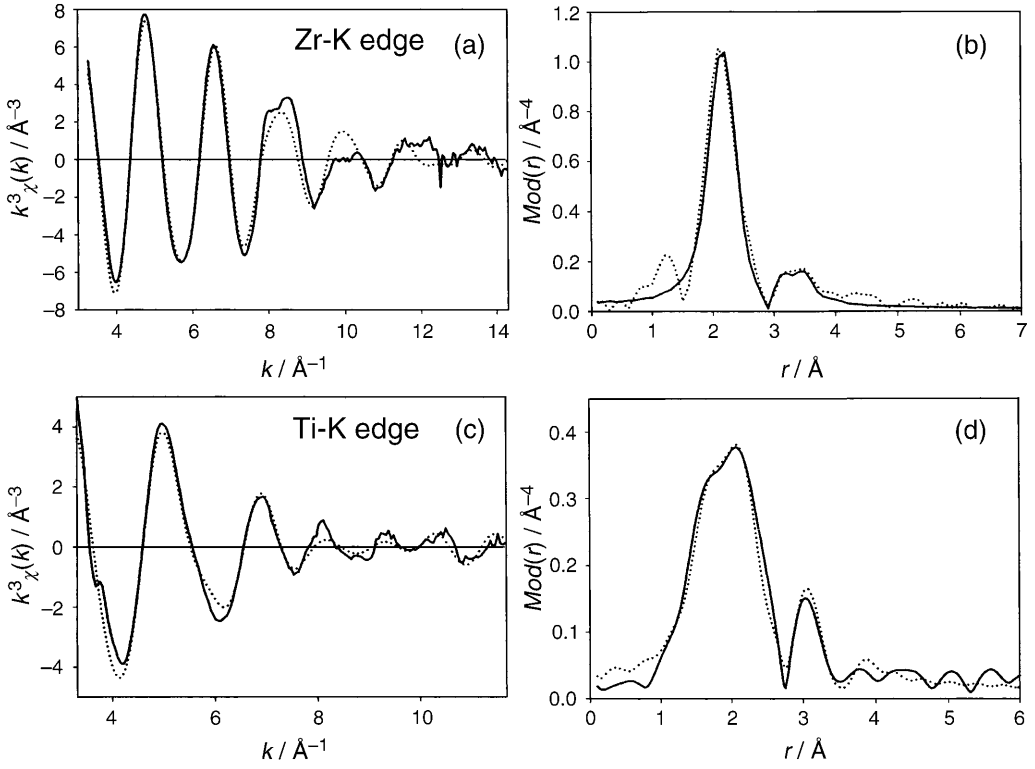

Fig. 5. Experimental (solid line) and calculated (dotted line) $k^3\chi(k)$ functions (a, c) and their *Fourier* transforms (b, d) of the $Ti_4Zr_4O_6(OBu)_4(OMc)_{16}$ cluster copolymerized with styrene (ratio 1:100) at the Zr–K (a, b) and Ti–K edge (c, d)

data from the crystals shows a good agreement with the diffraction studies. However, Zr–Ti and Ti–Ti distances were longer than in the crystal structure data as already observed for the Zr–K edge.

Nanocomposites of this cluster with poly(methacrylic acid), poly(methylmethacrylate), and polystyrene in 1:50 and 1:100 molar ratios were prepared. Altogether, the EXAFS studies reveal that in all samples the structure of the incorporated cluster is retained (Fig. 5). No influence of the type of polymer or the cluster-to-monomer ratio was observed.

The *Fourier* transforms of the Ti–K edge spectra shows that the function of the crystalline cluster exhibits a pronounced double peak (Fig. 4d), whereas the corresponding function of the copolymerized cluster has only a single, but broad peak (Fig. 5d). This qualitative result is also confirmed quantitatively. All *Debye-Waller*-like factors of the copolymerized clusters, independent of the type and ratio of the polymer, are larger than the corresponding values of the crystalline cluster, thus indicating an increase of the static disorder in the copolymerized phase.

Ti_2Zr_4 cluster

In $Ti_2Zr_4O_4(OBu)_2(OMc)_{14}$ the zigzag chain is terminated by two oxotitanium polyhedra (Fig. 6).

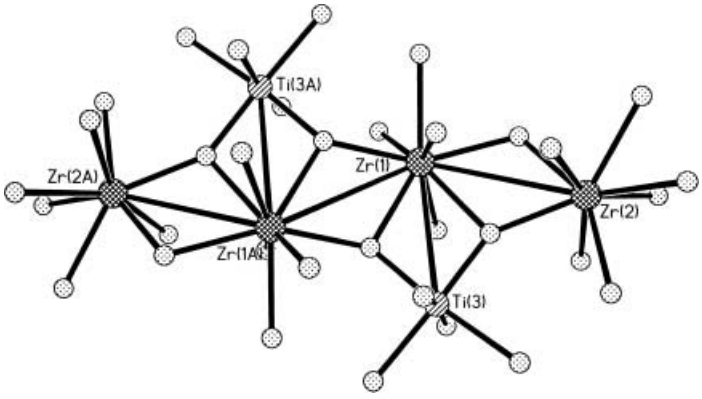

Fig. 6. Representation of the core of the $Ti_2Zr_4O_4(OBu)_2(OMc)_{14}$ cluster from X-ray structure analysis [16]

Table 4. Structural parameters of the $Ti_2Zr_4O_4(OBu)_2(OMc)_{14}$ cluster (pure as well as copolymerized with methacrylic acid (*MA*) and methylmethacrylate (*MMA*) in different ratios) as determined from the Zr–K edge EXAFS spectrum; the coordination numbers were fixed according to the averaged crystallographic values; for symbols, cf. Table 1

		r/Å	N	σ/Å	ΔE_0/eV	k-range/Å^{-1} Fit-index
Ti_2Zr_4 cluster,	Zr–O	2.20±0.02	8	0.086	20.1	3.10–14.20
crystalline	Zr–Ti	3.13±0.03	0.5	0.066		26.9
	Zr–Zr	3.54±0.04	1.5	0.073		
Ti_2Zr_4 cluster,	Zr–O	2.20±0.02	8	0.098	19.8	3.10–14.20
MA ratio 1:50	Zr–Ti	3.15±0.03	0.5	0.074		27.8
	Zr–Zr	3.52±0.04	1.5	0.094		
Ti_2Zr_4 cluster,	Zr–O	2.20±0.02	8	0.098	19.8	3.10–14.20
MA ratio 1:100	Zr–Ti	3.14±0.03	0.5	0.074		27.9
	Zr–Zr	3.52±0.04	1.5	0.094		
Ti_2Zr_4 cluster,	Zr–O	2.19±0.02	8	0.100	19.4	3.10–14.20
MMA ratio 1:50	Zr–Ti	3.18±0.03	0.5	0.073		23.3
	Zr–Zr	3.50±0.04	1.5	0.103		
Ti_2Zr_4 cluster,	Zr–O	2.20±0.02	8	0.100	19.0	3.20–14.30
MM ratio 1:100	Zr–Ti	3.17±0.03	0.5	0.077		28.2
	Zr–Zr	3.52±0.04	1.5	0.093		
Ti_2Zr_4 cluster,	Zr–O	2.20	8			
XRD [16]	Zr–Ti	3.11	0.5			
	Zr–Zr	3.51	1.5			

EXAFS analysis confirms the averaged first shell of the Zr atoms that is best described by 8 O atoms at 2.20 Å, 0.5 Ti atoms at 3.11 Å, and 1.5 Zr atoms at 3.51 Å (Table 4). The data obtained from the Zr–K edge proved, as already shown for the other nanocomposite samples, that the incorporated cluster did not structurally change in the polymer matrix. Only crystalline samples of the Ti_2Zr_4

cluster were studied at the Ti–K edge and showed good agreement with diffraction experiments (2 O atoms at 1.82 Å, 4 O atoms at 2.01 Å, and 1 Ti atom at 3.11 Å; Table 5). The comparison of the corresponding EXAFS functions (Figs. 4 and 7) additionally reveals that the environment of the metal atoms in the Ti_2Zr_4 and the Ti_4Zr_4 cluster cores are very similar.

Table 5. Structural parameters of the pure $Ti_2Zr_4O_4(OBu)_2(OMc)_{14}$ cluster as determined from the Ti–K edge EXAFS spectrum; the coordination numbers were fixed according to the averaged crystallographic values; for symbols, cf. Table 1

		r/Å	N	σ/Å	ΔE_0/eV	k-range/Å^{-1} Fit-index
Ti_2Zr_4 cluster,	Ti–O	1.83±0.02	2	0.090±0.014	17.1	3.50–13.00
crystalline	Ti–O	2.04±0.02	4	0.102±0.015		35.5
	Ti–Zr	3.13±0.03	1	0.095±0.014		
Ti_2Zr_4 cluster,	Ti–O	1.82	2			
XRD [16]	Ti–O	2.01	4			
	Ti–Zr	3.11	1			

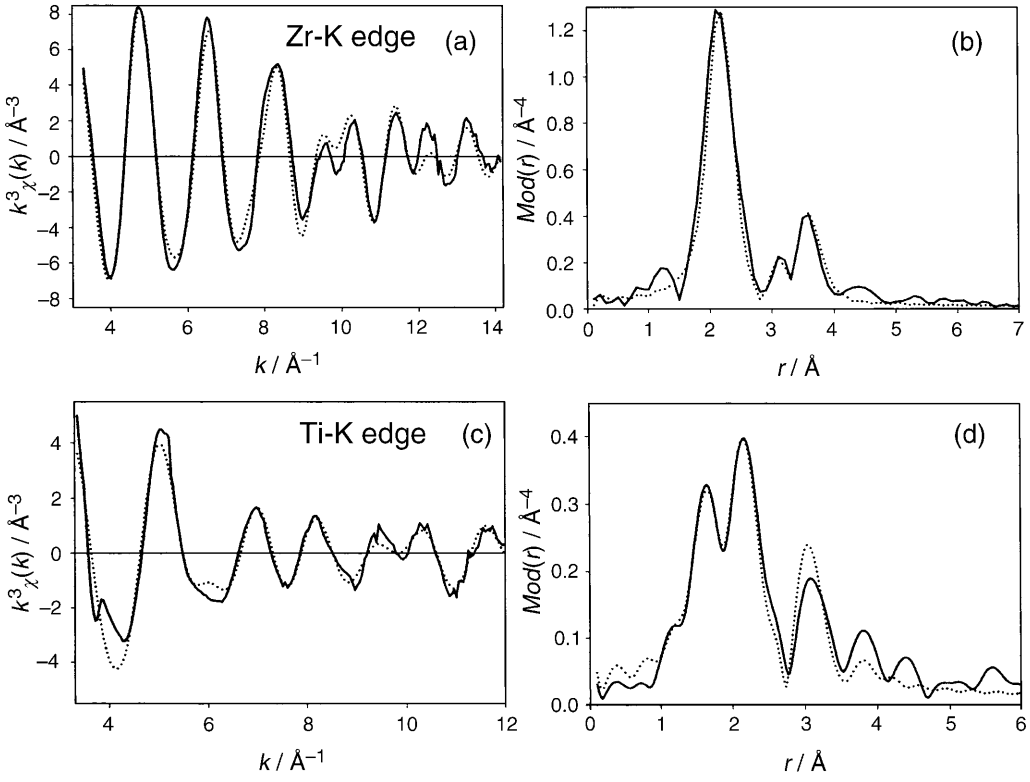

Fig. 7. Experimental (solid line) and calculated (dotted line) $k^3\chi(k)$ functions (a, c) and their *Fourier* transforms (b, d) of the pure $Ti_2Zr_4O_4(OBu)_2(OMc)_{14}$ cluster at the Zr–K (a, b) and Ti–K edge (c, d)

Conclusions

Surface-modified oxometallate clusters of Ti and Zr were investigated by EXAFS. Good agreement between crystallographic data of molecular structures and the EXAFS-analyzed systems was achieved. The analysis of nanocomposites of the clusters in different hybrid polymers reveals that the clusters are still intact in these materials, independent of the shape and composition of the cluster and also independent of the polymer type. However, in cases where the polymers can interact with the metal centers, exchange reactions of ligands with pending functionalities at the polymer chains cannot be excluded.

Experimental

Sample preparation

Surface-modified zirconium and titanium as well as mixed zirconium/titanium clusters were prepared as described in the literature [12, 16]. The nanocomposites were synthesized following a known procedure [18, 19].

EXAFS measurements and analysis

The EXAFS measurements of the samples were performed at the beamlines X1.1 (RÖMO II) and E4 at the *Hamburger Synchrotronstrahlungslabor* (HASYLAB) at DESY (Hamburg, Germany).

For the measurements at the titanium K-edge (4965.0 eV) a Si(111) double crystal monochromator and for the measurements at the zirconium K-edge (17998.0 eV) a Si(311) double crystal monochromator was used. The synchrotron beam current was between 80–140 mA (positron energy 4.45 GeV). All experiments were carried out at 25°C. In the case of the experiments at the Ti–K edge, the sample chamber was evacuated to a pressure below 10^{-4} mbar to grant a good signal-to-noise ratio. The experiments at the Zr–K edge were carried out under ambient conditions. The tilt of the second monochromator crystal was set to 30% harmonic rejection. Energy resolution was estimated to be about 1 eV for the Ti–K edge and 5 eV for the Zr–K edge. Data were collected in the transmission mode with ion chambers which were filled with nitrogen in the case of the measurements at the Ti–K edge (beamline E4) and with argon in the case of the measurements at the Zr–K edge (beamline X1.1). Energy calibration was performed with the corresponding metal foils.

In the case of the measurements at the titanium edge, the samples were embedded in a polyethylene matrix and pressed to pellets. The samples for the Zr–K edge measurements were prepared without polyethylene. The concentrations of all samples were adjusted to yield an absorption jump of $\mu \approx 1.5$. Data evaluation started with background absorption removal from the experimental absorption spectrum by subtraction of a *Victoreen*-type polynomial. Then the background-subtracted spectrum was convoluted with a series of increasingly broader *Gauss* functions, and the common intersection point of the convoluted spectra was taken as energy E_0 [22, 23]. To determine the smooth part of the spectrum corrected for pre-edge absorption, a piecewise polynomial was used. It was adjusted in such manner that the low-R components of the resulting *Fourier* transformation were minimal. After division of the background-subtracted spectrum by its smooth part, the photon energy was converted to photoelectron wave numbers k. The resulting EXAFS function was weighted with k^3. Data analysis in the k-space was performed according to the curved wave multiple scattering formalism of the program EXCURV92 with XALPHA phase and amplitude functions [24]. The mean free path of the scattered electrons was calculated from the imaginary part of the potential (VPI was set to -4.00), and an overall energy shift (ΔE_0) was assumed. The amplitude reduction factor (*AFAC*) was set to a value of 0.8 in the case of the Ti–K as well as the Zr–K edge.

Acknowledgments

We wish to thank HASYLAB at DESY, Hamburg, for the kind support of the synchrotron experiments at the beamlines E4 and A1, the *Fonds zur Förderung der wissenschaftlichen Forschung* (FWF), Austria, and the *Jubiläumsfonds der Stadt Wien* for financial support. This work was further supported by the IHP-Contract HPRI-CT-1999-00040 of the European Commission.

References

[1] Pomagailo AD (1997) Russ Chem Rev **66**: 679
[2] Pomogailo AD (2000) Russ Chem Rev **69**: 53
[3] Kickelbick G, Schubert U (2001) Monatsh Chem **132**: 13
[4] Kickelbick G, Progr Polym Sci (submitted)
[5] Schubert U (2001) Chem Mater **13**: 3487
[6] Bourgeat-Lami E, Espiard P, Guyot A, Briat S, Gauthier C, Vigier G, Perez J (1995) ACS Symp Ser **585**: 112
[7] Bourgeat-Lami E, Espiard P, Guyot A (1995) Polymer **36**: 4385
[8] Bourgeat-Lami E, Espiard P, Guyot A, Gauthier C, David L, Vigier G (1996) Angew Makromol Chem **242**: 105
[9] Bourgeat-Lami E, Lang J (1998) J Colloid Interface Sci **197**: 293
[10] Bourgeat-Lami E, Lang J (1999) J Colloid Interface Sci **210**: 281
[11] Bourgeat-Lami E, Lang J (2000) Macromol Symp **151**: 377
[12] Kickelbick G, Schubert U (1997) Chem Ber **130**: 473
[13] Kickelbick G, Schubert U (1998) Eur J Inorg Chem 159
[14] Kickelbick G, Wiede P, Schubert U (1999) Inorg Chim Acta **284**: 1
[15] Kickelbick G, Schubert U (1999) J Chem Soc, Dalton Trans 1301
[16] Moraru B, Kickelbick G, Schubert U (2001) Eur J Inorg Chem 1295
[17] Moraru B, Gross S, Kickelbick G, Trimmel G, Schubert U (2001) Monatsh Chem **132**: 993
[18] Moraru B, Hüsing N, Kickelbick G, Schubert U, Fratzl P, Peterlik H, Chem Mater (submitted)
[19] Trimmel G, Fratzl P, Schubert U (2000) Chem Mater **12**: 602
[20] Bertagnolli H, Ertel TS (1994) Angew Chem Int Ed Engl **1994**: 45
[21] Moraru B, Kickelbick G, Battistella M, Schubert U (2001) J Organomet Chem **636**: 172
[22] Ertel TS, Bertagnolli H, Hückmann S, Kolb U, Peter D (1992) Appl Spectrosc **46**: 690
[23] Newville M, Livins P, Yakoby Y, Rehr JJ, Stern EA (1993) Phys Rev B **47**: 14126
[24] Gurman SJ, Binsted N, Ross I (1986) J Phys **C 19**: 1845

Received October 23, 2001. Accepted November 12, 2001

Verleger: Springer-Verlag KG, Sachsenplatz 4–6, A-1201 Wien. – Herausgeber: Österreichische Akademie der Wissenschaften, Dr.-Ignaz-Seipel-Platz 2, A-1010 Wien, und Gesellschaft Österreichischer Chemiker, Eschenbachgasse 9, A-1010 Wien. – Redaktion: Währinger Straße 38, A-1090 Wien. – Satz und Umbruch: Thomson Press Ltd., New Delhi, India. – Offsetdruck: Manz Crossmedia, A-1051 Wien. – Verlagsort: Wien. – Herstellungsort: Wien. – Printed in Austria.